Eur. Phys. J. E (2016) **39**: 3
DOI 10.1140/epje/i2016-16003-0

THE EUROPEAN PHYSICAL JOURNAL E

Regular Article

Water activity in lamellar stacks of lipid bilayers: "Hydration forces" revisited

R. Leite Rubim[1,2], B.B. Gerbelli[1], K. Bougis[1,2], C.L. Pinto de Oliveira[1], L. Navailles[2], F. Nallet[2,a], and E. Andreoli de Oliveira[1]

[1] Universidade de São Paulo, Instituto de Física-GFCx, P.O.B. 66318, São Paulo, SP 05314-970, Brazil
[2] Université de Bordeaux, Centre de recherche Paul-Pascal–CNRS, 115 avenue du Docteur-Schweitzer, F-33600 Pessac, France

Received 22 September 2015 and Received in final form 13 November 2015
Published online: 25 January 2016 –

Abstract. Water activity and its relationship with interactions stabilising lamellar stacks of mixed lipid bilayers in their fluid state are investigated by means of osmotic pressure measurements coupled with small-angle X-ray scattering. The (electrically neutral) bilayers are composed of a mixture in various proportions of lecithin, a zwitterionic phospholipid, and Simulsol, a non-ionic cosurfactant with an ethoxylated polar head. For highly dehydrated samples the osmotic pressure profile always exhibits the "classical" exponential decay as hydration increases but, depending on Simulsol to lecithin ratio, it becomes either of the "bound" or "unbound" types for more water-swollen systems. A simple thermodynamic model is used for interpreting the results *without* resorting to the celebrated but elusive "hydration forces".

1 Introduction

From mixtures of lipids and water, multilamellar systems may naturally emerge. In such self-assembled systems, a periodic structure is formed by stacking lipid bilayers and layers of water. In the case where there is no in-plane order in the bilayers —in their so-called "fluid state"— the system exhibits the symmetry of a smectic A phase, commonly referred to as a lamellar L_α phase in the context of lipid materials [1].

Assessing the mechanisms responsible for the stability of such lamellar structures has been the core motivation for quite a large number of experimental or theoretical studies, with "hydration interactions" [2], on one hand, and "undulation interactions" [3] on the other hand, emerging as central concepts more than 35 years ago when direct electrostatic interactions are irrelevant. Techniques of choice for studying inter-bilayer interactions include osmotic pressure control [2, 4, 5], line-shape analysis in high-resolution [6] or grazing-incidence small-angle scattering geometries [7], dynamic light scattering [8], and "direct" methods with, *e.g.* Surface Force Apparatuses [9]. Clear experimental evidences have been obtained as regards undulation interactions in the swollen end of dilution lines [6], while the other (highly dehydrated) limit has often been generically characterised in terms of "hydration interactions" from the observed exponentially decaying force (or pressure) profile with natural scale 0.2–0.4 nm [2].

Here, we study a lecithin-based lamellar system in the presence of a non-ionic co-surfactant, a system which has shown its ability to efficiently encapsulate DNA fragments in spite of the absence of any obvious direct electrostatic mechanism at play [10–12]. The co-surfactant we use is an ethoxylated fatty acid, *i.e.* a (short) non-ionic block copolymer with amphiphilic properties. The present work therefore somehow expands ref. [13, 14], the focus being now *osmotic pressure control* instead of line-shape analysis in small-angle scattering.

The lamellar structure of the stacked bilayers is equilibrated with various semi-dilute (aqueous) solutions of polymers, which gives a handle on water activity (or, equivalently, osmotic pressure Π), while the stacking period ℓ is determined by means of small-angle X-ray scattering, following the method popularised by V.A. Parsegian [5]. Other relevant quantities are commonly manipulated when presenting or discussing the results, namely the bilayer volume fraction ϕ and the interfacial area per (average) amphiphilic molecule $\bar{\Sigma}$. Assuming homogeneous and ideally flat bilayers, a simple geometric description of the lecithin-Simulsol lamellar stack in water gives (see, *e.g.*, ref. [14])

$$\ell = 2\frac{\bar{v}}{\bar{\Sigma}} \times \frac{1}{\phi}\,, \tag{1}$$

where $\bar{v}$ is the effective molecular volume $xv_S + (1-x)v_L$ of the bilayer species (with v_L, respectively v_S, being the molecular volume of the lecithin, respectively, Simulsol molecules and x the Simulsol mole fraction in the bilayer), $\bar{\Sigma}$ similarly being an effective interfacial molecular area

[a] e-mail: nallet@crpp-bordeaux.cnrs.fr

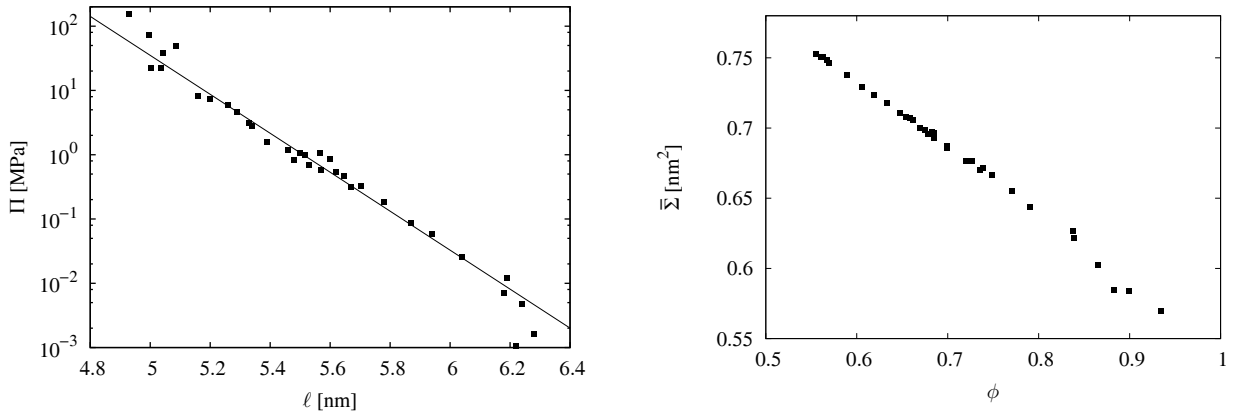

(a) Osmotic pressure Π (b) Lipid interfacial area $\bar{\Sigma}$

Fig. 1. (a) Lamellar stack equation of state. Note the quasi-exponential decay of osmotic pressure with stacking period ℓ: continuous line. Decay length *ca.* 0.143 nm. (b) Bilayer equation of state. Dehydration results in a *decrease* in optimal interfacial area per lipid molecule. Redrawn from data for egg lecithin in ref. [5].

$x\Sigma_S + (1-x)\Sigma_L$ derived from actual Simulsol Σ_S and lecithin Σ_L interfacial areas. Note that, while Π, ℓ, x or ϕ are experimentally well-defined quantities, and v_L, as well as v_S, can safely be considered as *constant* parameters, $\bar{\Sigma}$ is *model-dependent*, as should be clear from the assumptions leading to eq. (1): These assumptions would be spoilt by the presence of numerous structural defects (holes across single bilayers, passages connecting adjacent bilayers —implying no longer homogeneous bilayers), or large-amplitude area-storing bilayer undulations— implying no longer flat bilayers.

2 Thermodynamic considerations

2.1 Lamellar stacks

Implicitly assuming for the sake of simplicity a two-component (lipid-water) system, it is customary to cast the interpretation framework of the $\Pi(\ell)$ data into the mould of, loosely speaking, an inter-bilayer interaction potential energy per unit bilayer area V, but perhaps more rigorous (as already noticed in ref. [5]) to start from the excess *free energy* of the bilayer stack. Per unit volume of the lamellar stack (and disregarding an obvious dependence on temperature that remains implicit in the following), the excess free energy is a function of two among the three quantities appearing in eq. (1). Choosing ϕ and $\bar{\Sigma}$, the excess free energy density, formally written as follows:

$$f_{\rm exc}(\phi, \bar{\Sigma}) \tag{2}$$

should be zero, by definition, for either $\phi = 0$ or $\phi = 1$. The total Gibbs free energy is then expressed as

$$G = (N_w v_w + N_l \bar{v}) \left[p + \frac{\mu_w^+}{v_w}(1-\phi) + \frac{\mu_l^+}{\bar{v}}\phi + f_{\rm exc}(\phi, \bar{\Sigma}) \right]. \tag{3}$$

Here, p is the (hydrostatic) pressure. Indices w, respectively l, refer to water, resp. "average" lecithin/Simulsol lipid. The total numbers of molecules of a given species are N_w and N_l, and the chemical potentials for the *pure* species are μ_w^+ and μ_l^+. The lipid volume fraction is $\phi = N_l\bar{v}/(N_w v_w + N_l \bar{v})$. Incompressibility is enforced by considering the molecular volumes v_w and $\bar{v}$ as constant parameters, with therefore $\partial G/\partial p = N_w v_w + N_l \bar{v}$.

The "dilution law", namely the $\ell(\phi)$ relation, is derived from eq. (1) once the optimal interfacial area is obtained, for a given composition ϕ, by solving the minimisation equation

$$\frac{\partial G}{\partial \bar{\Sigma}} = 0, \tag{4}$$

which is equivalent to solving

$$\frac{\partial f_{\rm exc}}{\partial \bar{\Sigma}} = 0. \tag{5}$$

The "bilayer equation of state", that is to say the explicit solution to this latter equation, is commonly expressed as $\bar{\Sigma}(\phi)$ or $\bar{\Sigma}(\ell)$ relations.

The "lamellar stack equation of state" results from equating the water chemical potential in a lamellar stack of given composition ϕ—and, therefore, of given optimal interfacial area $\bar{\Sigma}(\phi)$—submitted to the (hydrostatic) pressure $p + \Pi$ to the pure water chemical potential when pure water is submitted to (hydrostatic) pressure p. The resulting standard expression is

$$\Pi = \phi \frac{\partial f_{\rm exc}}{\partial \phi} - f_{\rm exc}, \tag{6}$$

either expressed as a $\Pi(\phi)$ or a $\Pi(\ell)$ relation.

Examples of the two above-mentioned equations of state are given for illustration in fig. 1(a) and (b)—data extracted from ref. [5]. The quasi-exponential decay of the osmotic pressure Π with stacking period ℓ is also observed when Π is plotted against the thickness of the water channel $\ell_w \equiv \ell(1-\phi)$, though with a different decay length: A value *ca.* 0.256 nm is found in the latter case [5], instead of *ca.* 0.143 nm in fig. 1(a). Quite significant also is the

decrease in optimal interfacial area per lipid molecule $\bar{\Sigma}$ as dehydration proceeds, a feature already observed more than 50 years ago with surfactant-water or lipid-water systems [15–17].

In the quite common case where a phase coexistence between a lamellar structure with finite spacing $\ell_{\max}$ and (almost) pure water when added in excess is observed, the lamellar stack is said to be "bound". This amounts to saying that, at some "dilution limit", there is a finite value ϕ^* for the lipid volume fraction where the osmotic pressure reaches zero: $\Pi(\phi^*) = 0$. In the system studied in ref. [5], for instance, the dilution limit is found at about $\ell_{\max} = 6.25\,\mathrm{nm}$. At contrast, (less common) "unbound" systems may be swollen seemingly indefinitely with water, and $\phi^* \to 0$ or, equivalently, $\ell_{\max} \to +\infty$. The so-called "unbinding transition", theoretically described in refs. [18–20], separates "bound" systems, with somehow weak undulation interactions, from "unbound" systems where stronger undulation interactions overcome attractive, van der Waals forces. It has been experimentally evidenced in appropriately chosen lamellar systems, see for instance ref. [14] for a recent report.

2.2 Simple fluids

As argued in more details in this Section, the above-described unbinding features of lamellar stacks upon addition of solvent have actually some similarities with the liquid-gas transition in pure compounds when hydrostatic pressure is isothermally decreased: Molecular (translational) kinetic energy (3D configurational entropy) then plays the role of bilayer undulations in lamellar stacks (1D configurational entropy), with cohesive forces —viz. van der Waals interactions— acting similarly in both cases. Close to the triple point temperature, the liquid phase may be said to be "bound" in the sense that pressure may be decreased to (almost) zero while keeping a rather small specific volume for the system. Close to the critical point temperature, however, the liquid phase would be characterised as "unbound" because the specific volume may reach large values *even though* a significant pressure is still applied to the fluid. Figure 2 illustrates this very common behaviour in the case of the fluid phase of ethane—data extracted from ref. [21]—where, for the sake of comparison with lamellar phase data, the physically-relevant parameter, namely the specific volume, has been expressed as an average *distance* ℓ between neighbouring molecules in the liquid.

A conspicuous feature of the experimental pressure equations of state displayed in fig. 2 may be noted at the *high* pressure end of the two curves, with a quasi-exponential behaviour $p(\ell) \propto \exp(-\ell/\Lambda)$ that somehow resembles the one observed in fig. 1(a). At contrast with lamellar phase data, however, the characteristic decay length Λ is here *very short*. Values in the range 0.02–0.024 nm are found for Λ, the shorter value being appropriate for the lower temperature.

Interpreting parameter Λ in terms of molecular dimensions seems difficult, but a simple interpretation for the observed behaviour is easily found in considering the van der Waals equation of state for pure, fluid compounds. In terms of only two parameters, namely a second virial coefficient b_2 describing the intermolecular interactions, and an excluded volume v_0 accounting for the finite molecular dimensions, van der Waals equation of state is [22]

$$\frac{pv_0}{k_BT} = \frac{1}{2}\frac{b_2}{v_0}\left(\frac{v_0}{v}\right)^2 + \frac{v_0/v}{1-\frac{v_0}{v}}\,, \tag{7}$$

with v the specific volume of the van der Waals fluid, k_B the Boltzmann constant and T the temperature. Dense fluids, *i.e.* systems with specific volumes only moderately larger than v_0, may be obtained at moderate pressures if the second virial coefficient b_2 is *negative* enough. With the integral expression for b_2 in terms of the Mayer function [23], this occurs when k_BT, a measure of thermally driven translational kinetic energy, is small enough compared to cohesive energy. Below a critical temperature T_c where b_2 decreases below the condensation threshold $-27v_0/4$ in the van der Waals model, *liquid* phases may indeed be formed. An illustration is given in fig. 3 for two values of the second virial coefficient, one close to, the other one farther below the condensation threshold. Note that, for plotting eq. (7) in fig. 3, the specific volume range has been restricted: On the low density end, to avoid entering the liquid-gas coexistence region where eq. (7) no longer applies, but also on the high density end, to avoid

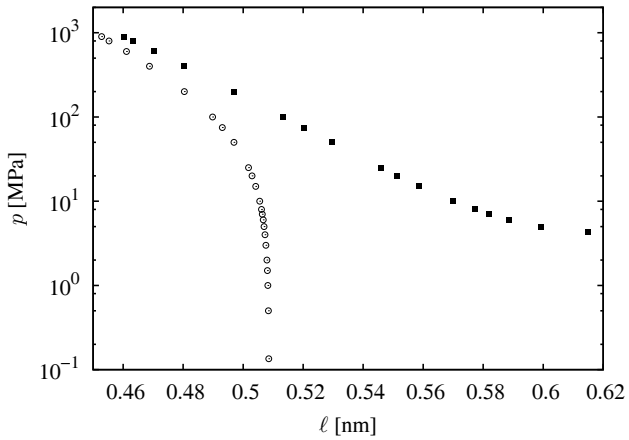

Fig. 2. Pressure equations of state for *liquid* ethane extracted from ref. [21], expressed as a function of $\ell \equiv \frac{\sqrt{2}}{2}(\frac{4M}{\rho N_A})^{1/3}$, at two temperatures $T = 190\,\mathrm{K}$ (⊙) and $T = 300\,\mathrm{K}$ (■). For pure ethane, triple point and, respectively, critical point temperatures and pressures are $T_t = 90.4\,\mathrm{K}$ and $p_t = 1.14\,\mathrm{Pa}$, respectively $T_c = 305.3\,\mathrm{K}$ and $p_c = 4.93\,\mathrm{MPa}$. The ℓ variable would be the nearest-neighbour distance if the mass density ρ of liquid ethane were obtained by placing molecules at the nodes of a face-centred cubic lattice. The molar mass of ethane is $M = 30.07\,\mathrm{g/mol}$ and N_A is the Avogadro constant. Note the quasi-exponential decay of pressure for small intermolecular separations-decay lengths *ca.* 0.020 nm ($T = 190\,\mathrm{K}$) and 0.024 nm ($T = 300\,\mathrm{K}$).

a spurious logarithmic singularity implicit in the van der Waals description of the configurational entropy.

The similarity between figs. 2 and 3 is striking, in particular as regards the large mismatch between decay parameters, resulting from either experiment or model, and characteristic molecular dimensions. A compelling interpretation for the quasi-exponential pressure decay observed over a range of intermolecular separations is therefore the following: It is not related to any structural property of the system and should be attributed to the standard competition (with a temperature-dependent outcome, obviously) between *cohesive* energy, favoured in high density states because of attractive van der Waals interactions between molecules (b_2 term in eq. (7)), and *configurational entropy*, reduced in high density states owing to short-range steric repulsions (v_0 term in eq. (7)). Besides, the precise *shape* of the interaction profile, *e.g.* a $1/\ell^{12}$ repulsive well combined with a $-1/\ell^6$ attractive component in the standard Lennard-Jones parametrisation of van der Waals interactions [24], is irrelevant here since the spatial integration of the Mayer function leading to b_2 smoothes out such details.

Taking one step further and considering the similarities between fig. 1(a) with either fig. 2 or fig. 3, it now seems natural to relate the quasi-exponential decay in the lamellar stack equation of state to a similar competition between cohesive energy (arising in lamellar stacks from van der Waals interactions through the water channels between lipid bilayers) and configurational entropy, as repeatedly suggested by J. Israelachvili and H. Wennerström [25–27]. This idea —in essence that "the swelling process is entropy driven" [28]— has found a partial support in recent numerical simulations [29]. It is developed in sect. 2.3 below.

2.3 Lamellar stacks "à la van der Waals"

Before presenting our model, a word of caution: Nothing prevents, in principle, some *direct* (repulsive) "hydration forces" playing a (marginal) role in the detailed characteristics of the lamellar stack equation of state. Possible physical mechanisms for such direct forces involve the solvent (water) binding properties with the bilayer surfaces [30], or solvent structural properties [31,32] through a mechanism similar to wetting [33] in this latter case: With *antisymmetric* boundary conditions at the bilayer-solvent interface, the order parameter profile of a (non-scalar) property associated to solvent across the water channel, electric polarisation typically, would lead indeed to an effective *repulsive* interaction in the lamellar stack. Interactions would nevertheless remain essentially attractive in the case of symmetric boundary conditions, as shown by Richetti *et al.* in their study of a structure-prone (presmectic) solvent confined between solid surfaces [34]. In any case, "hydration forces" if they exist in this restricted sense would merely affect the *magnitude* of the second virial coefficient in the van der Waals fluid analogy, increasing $|b_2|$ (if attractive—more cohesion) or decreasing $|b_2|$ (if repulsive—less cohesion), which would only slightly displace the location of the critical temperature in the phase diagram.

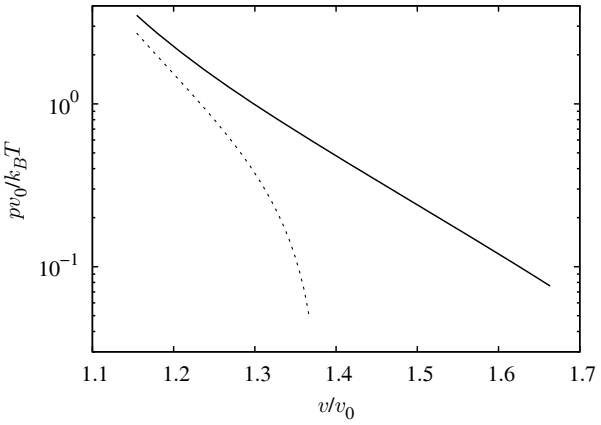

Fig. 3. Pressure equations of state in reduced units for the *liquid* phase of a van der Waals fluid. Second virial coefficients $b_2/v_0 = -10$ (dashed line) and -7.92 (continuous line). From the common tangent construct, the liquid-gas binodal begins, respectively, at the specific volumes $v_L \approx 1.37v_0$ and $v_L \approx 1.67v_0$. Note the quasi-exponential decay of pressure with decay parameters, respectively, $0.081v_0$ and $0.143v_0$.

It therefore appears necessary to reconsider carefully the interpretation of statements similar to

> *Hydration repulsion universally acts between well-solvated surfaces in water and balances the van der Waals attraction in the nanometre range*

(quoted from ref. [29]) found in references spanning more than 30 years, for instance refs. [5,18,35]. The underlying vision of a *balance* is commonly expressed in quantitative terms by adding pressures (forces per unit bilayer area), with as many contributions to the sum as identified interactions. In the simplest case where only hydration and van der Waals interactions are considered to be relevant, the total pressure is [5]

$$P(\ell) = P_0 \exp\left[-(\ell-\delta)/\lambda\right] - \frac{H}{6\pi}\left[\frac{1}{(\ell-\delta)^3} + \frac{1}{(\ell+\delta)^3} - \frac{2}{\ell^3}\right], \tag{8}$$

where the exponentially decaying, repulsive term represents hydration forces and the combination of power laws describes, in the simplest possible way, attractive van der Waals forces between identical, planar and parallel objects of infinite lateral extension and thickness δ ($\equiv 2\bar{v}/\bar{\Sigma}$ in eq. (1)), separated by a channel of width $\ell - \delta$. In eq. (8), $P_0 > 0$ is the amplitude of the hydration pressure, λ its decay length and $H > 0$ the Hamaker coefficient.

From ref. [5], values appropriate for describing the experimental measurements in egg-lecithin-based lamellar stacks are: $P_0 \approx 7.05 \times 10^8$ Pa, $\lambda \approx 0.256$ nm and $H \approx 6.0 \times 10^{-21}$ J. As already mentioned in sect. 2.2, parameter λ—introduced here—differs from parameter Λ used for describing the lamellar stack equation of state $\Pi(\ell)$ displayed in fig. 1(a). This comes from the choice made in ref. [5], the lamellar stack equation of state being represented by a *different* function $\Pi(\ell - \delta)$. It differs

from $\Pi(\ell)$ because δ actually depends on hydration. The "balance" between hydration and van der Waals forces is obtained at a maximum swelling $\ell_{\max} \approx 6.3\,\mathrm{nm}$, where bilayer thickness is $\delta \approx 3.5\,\mathrm{nm}$.

But there is more in thermodynamics than in mechanics or, in other terms, free energy is more than mere potential energy: A complete description of, *e.g.*, equations of state or phase diagrams is not wholly encapsulated in force models similar to eq. (8) that ignore entropy, a criticism already explicitly formulated in the context of the unbinding transition by R. Lipowski and S. Leibler [18] or S.T. Milner and D. Roux [20]. They showed that, even though the mechanical (but *ad hoc*) model, eq. (8), accounts extremely well for the measured osmotic pressure data—fig. 1(a)—it utterly fails in explaining the detailed thermodynamic features of the unbinding transition. What is missing in the naive mechanical approach is, specifically, a description of the *bilayer* equation of state—fig. 1(b)—as well as a physically well-grounded interpretation of the "hydration forces"—two aspects recently emphasised in ref. [35, 36] and [37], respectively.

In the present approach, we propose to overcome these shortcomings by modelling the fundamental thermodynamic quantity in the problem, namely the excess free energy density f_{exc}, with the following physical ingredients: i) Helfrich undulation (entropic) interactions between bilayers across the water channels, ii) van der Waals (and possibly other) *direct* interactions at the level of a second virial coefficient description as in ref. [20], and iii) bilayers described as being, individually, a kind of two-dimensional van der Waals fluid well *below* its own unbinding transition in the sense given to it in sect. 2.2. It is worth mentioning again that, owing to the virial approach chosen in ii), the precise *shape* of the interaction potential, a repulsive exponentially decaying term added to an attractive power-law contribution as would result from eq. (8) for instance, is irrelevant here, for the same reasons as given in sect. 2.2. In quantitative terms, our heuristic approach amounts to writing

$$\ell \times f_{\mathrm{exc}} = \frac{3\pi^2}{128}\frac{(k_BT)^2}{\kappa}\frac{1}{(\ell-\delta)^2} - k_BT\chi\phi^2\ell + \frac{k_BT}{\bar{\Sigma}}\ln\left[\frac{\varsigma^2}{e(\bar{\Sigma}-\Sigma_0)}\right] + \frac{1}{2}k_BT\frac{b_2}{\bar{\Sigma}^2}\,, \qquad (9)$$

where ℓ depends on $\bar{\Sigma}$ and ϕ according to eq. (1) and δ is again a convenient notation for $2\bar{v}/\bar{\Sigma}$. In eq. (9), e being the base of the natural logarithm, κ is the bilayer bending modulus (controlling the amplitude of thermally driven bilayer undulations [3]), χ is the second virial coefficient accounting for (inter-bilayer) direct interactions according to S.T. Milner and D. Roux [20], Σ_0 is the "excluded area" in the two-dimensional fluid of lipid molecules, b_2 is the second virial coefficient accounting for *intra-bilayer* interactions between lipid molecules, "*à la* van der Waals", and ς a parameter with length units analogous to the thermal de Broglie wavelength in ideal (3D) classical gases [38].

For illustrating the essential role of ingredient iii) in the physical content of eq. (9), fig. 4 displays a set of curves

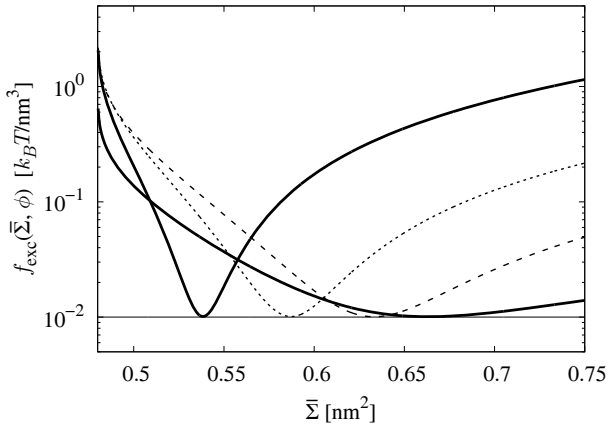

Fig. 4. Excess free energy per unit volume of a bilayer stack f_{exc}, according to the thermodynamic model eq. (9), drawn as a function of the area $\bar{\Sigma}$ per lipid molecule for a few selected values of the bilayer volume fraction: $\phi = 0.25$—rightmost continuous line, $\phi = 0.80$—dashed line, $\phi = 0.90$—dotted line, and $\phi = 0.95$—leftmost continuous line. Note that, for the sake of clarity, a ϕ-dependent constant has been added to f_{exc} to adjust the minimum of each curve to the (arbitrarily chosen) value $0.01\,k_BT/\mathrm{nm}^3$ (thin horizontal line). The shifts in free energy per unit volume are, along decreasing hydration, $\Delta \approx 0.46$, 1.43, 1.43 and $0.87\,k_BT/\mathrm{nm}^3$.

Table 1. Numerical values chosen for illustrating the properties of the thermodynamic model, eq. (9).

κ/k_BT	$\bar{v}$	Σ_0	ς	χ/ς^3	b_2/Σ_0
	[nm^3]	[nm^2]	[nm]	[nm^{-6}]	
2.	1.0	0.48	$\sqrt{\Sigma_0}$	0.1	-10

for f_{exc} as a function of the area $\bar{\Sigma}$ per lipid molecule for a few selected bilayer volume fractions ϕ. The numerical values for the parameters used in the computation of f_{exc} are given in table 1. As suggested by the trends observed in fig. 4 (and confirmed by a thorough numerical analysis), the "optimal" area where f_{exc} reaches its minimum value depends only weakly on the bilayer volume fraction ϕ for *dilute* lamellar stacks, but much more strongly as the lamellar phase becomes highly dehydrated. This is easily interpreted, in qualitative terms, by a competition between *stack* entropy, as described by the Helfrich undulation term that strives for *large* ℓ (corresponding to small $\bar{\Sigma}$) values, and *two-dimensional* liquid bilayer entropy, as described by the excluded area Σ_0 term, oppositely striving for large $\bar{\Sigma}$ values. The second virial coefficient b_2, negative enough to ensure a "bound" two-dimensional liquid state for the lipid fluid, comes into play when the stack entropy is optimised, *i.e.* for dilute enough lamellar stacks, and stabilises $\bar{\Sigma}$ to a value greater than, but still rather close to Σ_0 ($\approx 1.4 \times \Sigma_0$ for table 1 parameter values).

Even though it appears difficult to obtain the bilayer equation of state by analytically solving eq. (5), a numerical procedure for determining the optimal $\bar{\Sigma}(\phi)$ is easily implemented, considering the simple shapes of the f_{exc}

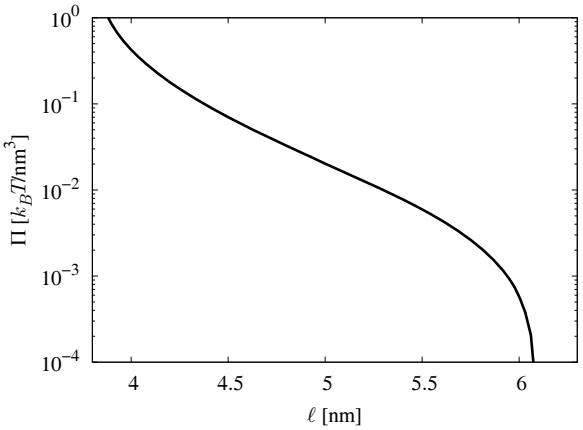

(a) Osmotic pressure Π

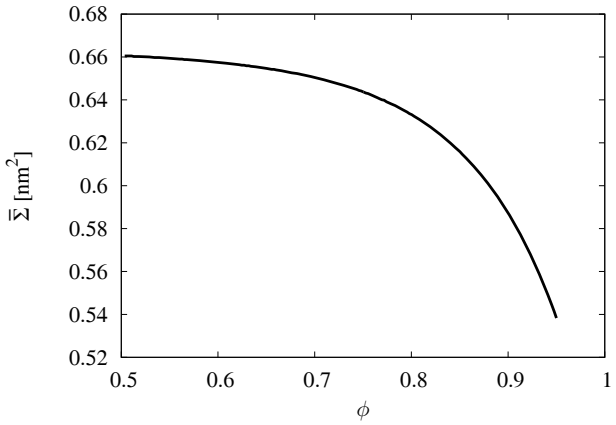

(b) Lipid interfacial area $\bar{\Sigma}$

Fig. 5. (a) Osmotic pressure Π of the lamellar stack as a function of the stacking period ℓ. The osmotic pressure reaches *ca.* 4 MPa when the lamellar phase is highly dehydrated. At the dilution limit $\ell_{\max} \approx 6.1$ nm, $\Pi \to 0$. There is a quasi-exponential decay of the osmotic pressure with a decay length ≈ 0.43 nm between these two limits. (b) Optimal area $\bar{\Sigma}$ per lipid molecule as a function of the bilayer volume fraction ϕ. Numerical results derived from the thermodynamic model eq. (9) with parameters given in table 1.

curves displayed in fig. 4. But the *possibility* of describing a "bound" lamellar stack, that is to say a system where the osmotic pressure Π reaches 0 at a *finite* hydration ϕ^* (sect. 2.1) should be simultaneously taken into account. This is not a too stringent constraint since eq. (6) leads in the context of the present model eq. (9) to a rather simple expression for the osmotic pressure, namely

$$\Pi = \frac{3\pi^2}{64}\frac{(k_BT)^2}{\kappa}\frac{1}{(\ell-\delta)^3} - k_BT\chi\phi^2, \qquad (10)$$

where the terms originating from the two-dimensional fluid of lipid molecules exactly cancel out. The resulting lamellar stack equation of state, as well as the bilayer equation of state are displayed in fig. 5(a) and (b), respectively. The broad features of both figures are rather similar to the experimental results displayed in fig. 1(a) and (b) for lamellar stacks, and (as far as the pressure equation of state is concerned) in fig. 2 for a simple fluid. In addition, the unbinding transition remains well described within the framework of eq. (9), extending ref. [20]. We have (numerically) explored the consequences on the dilution limit $\ell_{\max}$ of decreasing the Milner-Roux virial coefficient χ, keeping all other parameters fixed to the values given in table 1. As shown in fig. 6, the prediction of our model is compatible with a scaling law $\ell_{\max} \propto |\chi - \chi_c|^{-\alpha}$, with critical unbinding occurring for $\chi_c \approx 2.2 \times 10^{-6}$ nm^{-3} (or $k_BT\chi_c \approx 9.2$ Pa) and an unbinding exponent $\alpha \approx 0.9$. The discrepancy between our result for the unbinding exponent, namely $\alpha \approx 0.9$, and the theoretically predicted values $\psi = 1$ in ref. [20] or $\psi = 1.00 \pm 0.03$ in ref. [18] may come from the unsophisticated numerical methods used for obtaining the bilayer equation of state from eq. (5). We leave a more detailed discussion to interested specialists.

In sect. 3, we further strengthen the relevance of our thermodynamic model, confronted with experimental results obtained for lecithin-Simulsol lamellar phases of varying bilayer compositions.

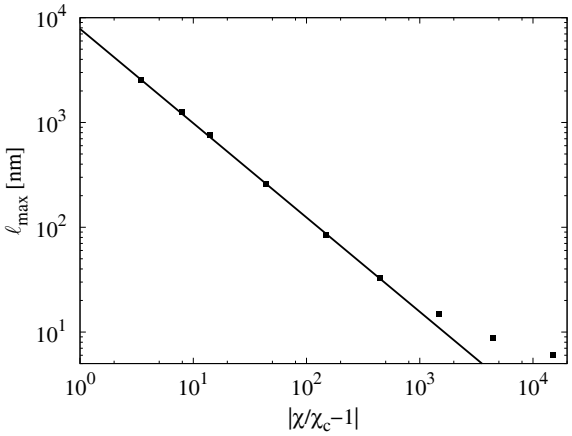

Fig. 6. Dilution limit $\ell_{\max}$ as a function of $|\chi/\chi_c - 1|$. The continuous line describes a power-law divergence of $\ell_{\max}$ as the Milner-Roux virial coefficient approaches the critical value χ_c, all other parameters in eq. (9) being kept fixed to the values given in table 1. The power-law divergence, with $k_BT\chi_c \approx 9.2$ Pa and $\alpha \approx 0.9$, is the expected signature of a critical unbinding transition occurring in the lamellar stack as direct inter-bilayer interactions become less attractive [20].

3 Experimental results and discussion

Small-angle X-ray scattering data are recorded, for a given bilayer composition x (described, from now on, in terms of Simulsol *mass* fraction, instead of mole fraction as in sect. 1), after immersing the dry lipid material in polymer solutions of various initial concentrations and waiting for water activity to equilibrate in both lamellar and polymer phases. Typical results are displayed in fig. 7, for a system with Simulsol mass fraction $x = 0.3$. The first and second order Bragg peaks, with ratio 1:2 as expected for a one-dimensional lamellar order, are always observed, a third order peak being also noticeable in the investigated

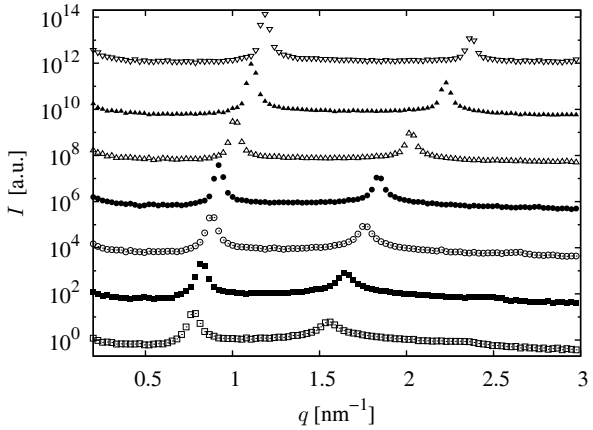

Fig. 7. Small-angle X-ray scattering data for a series of lamellar stacks with bilayer composition $x = 0.3$ in osmotic equilibrium with polymer solutions of increasing concentrations: $c_p = 0.068$ g/mL (⊡), 0.100 (■), 0.141 (⊙), 0.162 (●), 0.259 (△), 0.378 (▲), and 0.472 (▽). The stacking period ℓ decreases with increasing osmotic pressure.

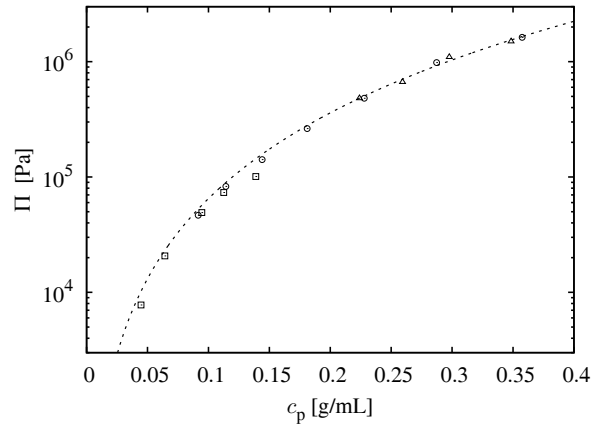

Fig. 8. Osmotic pressure as a function of polymer concentration for three series of polymer solutions differing by the polymer degrees of polymerisation. PVP10 (△) PVP40 (⊙) PVP360 (⊡). The dotted line is a polynomial fit, appropriate for semi-dilute polymer solutions, with equation $\Pi = 4 \cdot 10^6 \times c_p^2 \times (1 + 6.25 \times c_p)$; pressure in Pa, concentration in g/mL.

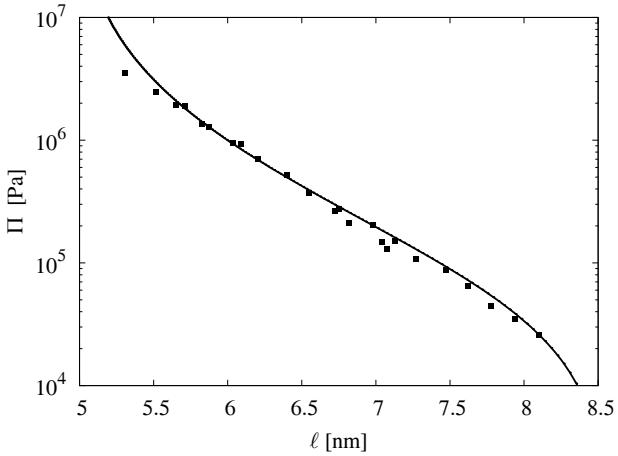

Fig. 9. Lamellar stack equation of state $\Pi(\ell)$ for the system with bilayer composition $x = 0.3$. Continuous line from model discussed in sect. 2.3, see text for details.

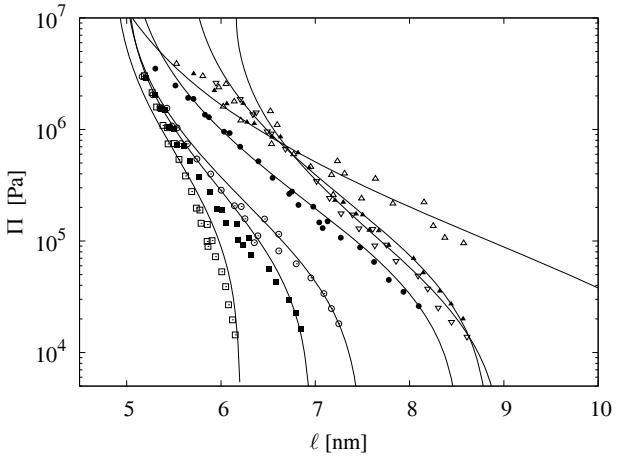

Fig. 10. Lamellar stack equations of state $\Pi(\ell)$ for systems with bilayer compositions $x = 0$ (⊡), $x = 0.05$ (■), $x = 0.1$ (⊙), $x = 0.3$ (●), $x = 0.5$ (△), $x = 0.7$ (▲) and $x = 0.8$ (▽). Continuous lines from model discussed in sect. 2.3, see text for details.

q-range for the more hydrated samples. The Bragg peaks are shifted towards larger values as osmotic pressure is increased because of the concomitant dehydration of the lamellar stack.

From the first order Bragg peak location q_0, the stacking period ℓ is directly obtained: $\ell = 2\pi/q_0$. Since the dilution law, *i.e.* the $\ell(\phi)$ relation, has been previously experimentally determined [13], the X-ray measurement indirectly gives the bilayer volume fraction ϕ. Because the amount of (initially dry) lipid in the whole system is known, mass conservation allows determining the *equilibrium* polymer concentration from its initial value in the known amount of polymer solution used for hydrating the lamellar stack. The lamellar stack equation of state then results from the auxiliary calibration curve (see fig. 8) giving the osmotic pressure Π of the polymer solution as a function of polymer concentration. An illustration for the system with Simulsol mass fraction $x = 0.3$ is given in fig. 9, with a quasi-exponential decay of the osmotic pressure observed in a range of stacking parameters ℓ.

The set of data shown in fig. 10 is obtained by repeating the same procedure and analyses for mass fractions spanning the pure lecithin ($x = 0$) to the almost pure Simulsol ($x = 0.8$) range. It was not possible to include the *pure* Simulsol system, and not even the $x = 0.9$ bilayer composition in the present study because at low osmotic pressures the water channel height reaches values so large that the polymer molecules can no longer be considered as *excluded* from the lamellar stack. Thus, increasing x

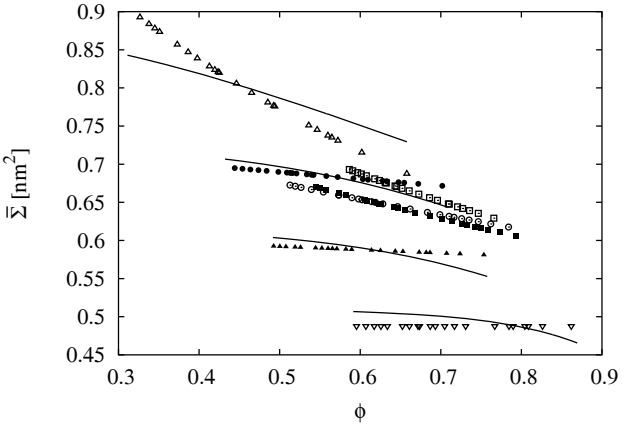

Fig. 11. Experimental (symbols) and selected model (continuous lines) bilayer equations of state $\bar{\Sigma}(\phi)$ for lamellar stacks with bilayer compositions $x = 0$ (⊡), $x = 0.05$ (■), $x = 0.1$ (⊙), $x = 0.3$ (●, —), $x = 0.5$ (△, —), $x = 0.7$ (▲, —) and $x = 0.8$ (▽, —).

Table 2. Numerical values chosen for describing experimental lamellar stack equations of state using eq. (9). Parameters $\bar{v}$ and b_2/Σ_0 kept constant to values $1.25\,\mathrm{nm}^3$ and -10, respectively. Parameter $\varsigma \equiv \sqrt{\Sigma_0}$. The last column gives the *model-predicted* dilution limits $\ell_{\max}$ that result from the chosen parameters.

x	κ/k_BT	χ/ς^3	Σ_0	$\ell_{\max}$
		[nm^{-6}]	[nm^2]	[nm]
0.8	0.55	0.18	0.370	9.01
0.7	0.15	0.43	0.477	8.86
0.5	0.047	0.43	0.635	12.0
0.3	0.13	0.43	0.525	8.53
0.1	0.33	0.30	0.495	7.51
0.05	0.40	0.36	0.485	6.95
0.0	0.35	0.65	0.505	6.22

apparently plays the role of approaching the unbinding transition here, as recently observed for a closely related system by a different technique [14].

The thermodynamic model discussed in sect. 2.3 and, more specifically, eq. (9) have been used for describing the lamellar stack equations of state displayed in figs. 9 and 10, as well as the bilayer equations of state displayed in fig. 11. We have not attempted to implement a complete fitting procedure to finely tune values for *all* the parameters listed in table 1, but checked in a few numerical simulations the influence of changing the bilayer bending modulus κ (bilayer stack entropy), as well as the Milner-Roux virial coefficient χ (bilayer stack enthalpy, resulting from both attractive and repulsive contributions to interbilayer *direct* interactions) and excluded area Σ_0 (two-dimensional fluid entropy). The continuous curves superimposed to data points in figs. 9 and 10 obviously give a fair description of the osmotic pressure data, with parameters given in table 2. The description, though acceptable, is less satisfactory as far as the bilayer equation of state is concerned, see fig. 11. Note that, for a better readability, a (representative) subset only of the available model curves is displayed. Improvements in the two-dimensional liquid model for describing the intra-bilayer thermodynamic contribution to the lamellar stack excess free energy, eq. (9), might here be required.

There is a rather remarkable trend in the evolution with the bilayer composition x of the model parameters κ, χ and Σ_0, as well as in the model-predicted dilution limit $\ell_{\max}$ illustrated in fig. 12(a), (b), (c), and (d), respectively. Two conspicuous compositions can be distinguished, one in the range $x = 0.05$–0.1 close to *pure* lecithin, and when x is close to 0.5. In a previous structural study of the same lecithin-Simulsol system [13], the value $x = 0.5$ was already experimentally evidenced as separating two regimes, even though the *experimental* dilution limit did not follow what is predicted here fig. 12(d). Still, the data for the area per (effective) lipid molecule $\bar{\Sigma}$ as a function of hydration displayed in fig. 11 clearly indicates that composition $x = 0.5$ experimentally plays a special role. The area per lipid molecule is significantly larger—and specially sensitive to hydration—than with all other bilayer compositions, an experimental feature independent from any model. This could indicate that the composition threshold for the "brush-to-mushroom" conformational transition in the hydrophilic blocks of Simulsol molecules suggested in ref. [13] and [14] is close to $x = 0.5$, and may give a clue for reaching a better agreement between experimental and predicted bilayer equations of state, at the expense of introducing a "brush-to-mushroom" variable into eq. (9). Besides, the experimental "back-and-forth" variation of $\bar{\Sigma}$ when x is close to zero observed in fig. 11, though not easily interpreted, is nicely compatible with the picture that emerges from the thermodynamic model of the lamellar stack, fig. 12, being simultaneously much less model-dependent: It should therefore correspond to a robust, but still unexplained, feature of the lecithin-dilute Simulsol mixture.

4 Conclusion

The interplay between soft confinement and steric effects has been studied in lamellar stacks of mixed lecithin-Simulsol bilayers, varying hydration and bilayer composition, by coupling osmotic pressure with small-angle X-ray scattering measurements that give access to both "lamellar stack" and "bilayer" equations of states.

With the help of a thermodynamic model of lamellar stacks that extends the approach of S.T. Milner and D. Roux [20] by the explicit inclusion of the thermodynamic properties of a two-dimensional fluid representing the lipid bilayers, we are able to quantitatively reproduce the osmotic pressure, and semi-quantitatively the lipid area data, keeping a meaningful description of the unbinding transition. The physical ingredients of the model are

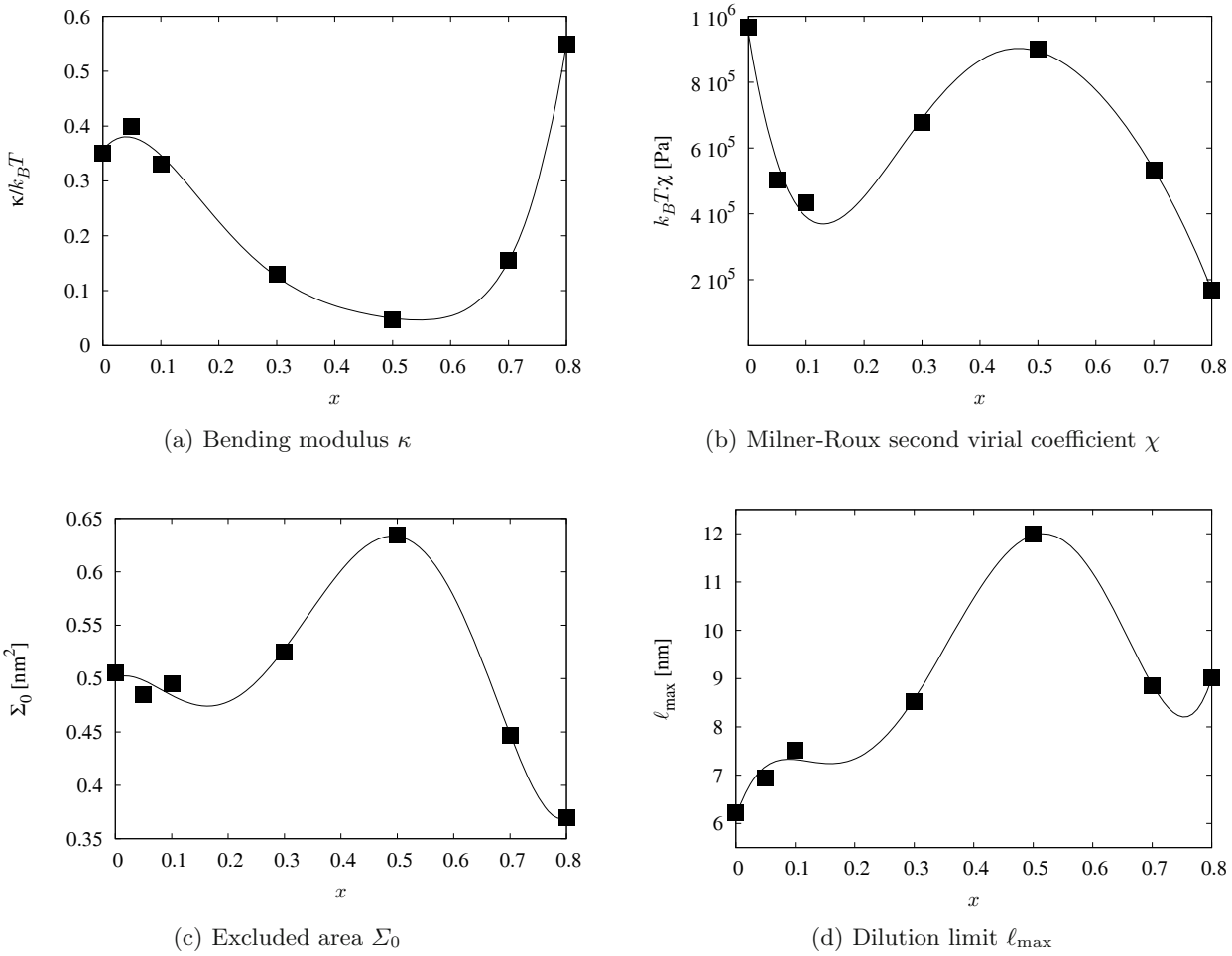

(a) Bending modulus κ

(b) Milner-Roux second virial coefficient χ

(c) Excluded area Σ_0

(d) Dilution limit $\ell_{\max}$

Fig. 12. Evolution as a function of bilayer composition x of the lamellar stack thermodynamic parameters. The continuous lines are guides for the eye. The bilayer configurational entropy is maximal close to $x = 0.5$ (panel a). Inter-bilayer attractive interactions are maximal and of comparable magnitude for $x = 0$ and $x = 0.5$ (panel b). The excluded area of the two-dimensional bilayer fluid is maximal close to $x = 0.5$ (panel c). The dilution limit of the lamellar stack is maximal close to $x = 0.5$ (panel d).

the Helfrich undulation interactions, controlled by a bending modulus parameter κ, *direct* inter-bilayer interactions controlled by the Milner-Roux virial coefficient χ, and a description of the two-dimensional lipid fluid by the venerable van der Waals model designed more than a century ago for ordinary fluids, with an excluded-area parameter Σ_0 and a second virial coefficient b_2. The celebrated, but elusive "hydration forces" play no role whatsoever in the model, while quasi-exponential osmotic pressure profiles remain, at least in a restricted range of water content in the lamellar stacks.

Among the intriguing outcomes of applying the model to describing the available osmotic and small-angle scattering data, it appears that adding a co-surfactant (Simulsol) to the lipid bilayer *not necessarily* always increases the bilayer flexibility, even though κ remains very sensitive to the amount of co-surfactant. This may be due to a kind of "brush-to-mushroom" transition taking place in the hydrophilic block of the Simulsol surfactant. The model prediction also does not quite fit with previous experimental results on the same system as far as the *dilution limit* of the lamellar stacks are concerned.

The better knowledge of the lamellar stack free energy gained here should still be refined, for instance in view of understanding the detailed mechanisms of the lamellar-lamellar phase coexistence at low hydration observed in rather similar lecithin-Simulsol systems [14].

Author contribution statement

All authors contributed equally to the present work.

The support by Fundação de Amparo à Pesquisa do Estado de São Paulo through grant 2011/16149-8 is gratefully acknowledged. We also thank IdEx Bordeaux (France) and Conselho Nacional de Desenvolvimento Científico e Tecnológico (Brazil) for providing support through their respective programs "Doctorat international" and "Ciência sem Fronteiras".

Appendix A.

Appendix A.1. Polymer solutions

The polymer used in this study is polyvinylpyrrolidone (PVP), from Sigma-Aldrich, in three molecular weights (10, 40 and 360 kg/mol). The polymer solutions are purified using snakeskin dialysis tubes (from Thermo Scientific) of different pore dimensions. The dialysis compartments filled with polymer solution were immersed in a tank initially containing pure water, and the water content was changed a few times, until the total volume reached 300 times the volume of the solution. The whole procedure took about one week. Once purified, the solutions were freeze-dried, which allowed re-dispersing the polymer material in water at various desired concentrations. The complete polymer dissolution could take a few days for the more concentrated solutions with PVP360.

The osmotic pressure of each prepared solution was measured with the PZL-100 osmometer from PZL Tecnologia Company. Results are displayed in fig. 8. The nearly quadratic increase of osmotic pressure with polymer concentration, independently of the polymer molar mass, is characteristic of polymer solutions being in their semi-dilute regime. The $\Pi(c_p)$ relation is empirically described by the polynomial law $\Pi = 4\cdot10^6 \times c_p^2 \times (1+6.25\times c_p)$ —pressure in Pa, concentration in g/mL— which allows computing the osmotic pressure applied to lamellar stacks.

Appendix A.2. Osmotically stressed lamellar stacks

The lipid membranes are prepared with soy lecithin (Avanti Polar Lipids) and a non-ionic commercial cosurfactant (Simulsol 2599 PHA, Seppic). Soy lecithin contains mainly dilinoleoylphosphatidylcholine (DLPC), with typically 35% of other (zwitterionic) lipids. Simulsol is a mixture of ethoxylated fatty acids (71% oleic and 11% palmitic acids being the main components), with an average of 10 CH_2–O–CH_2 groups in the hydrophilic block. Lecithin and Simulsol are co-solubilised in cyclohexane in desired proportions, which always leads to macroscopically homogeneous, transparent solutions. Therefore, *a priori* homogeneous mixtures of controlled composition (labelled as a mass fraction x) are obtained by evaporating the solvent. Lamellar systems are then prepared by swelling a chosen mass of the dry amphiphilic mixture with thrice the amount of polymer solutions, tuning the polymer mass and initial concentration to scan as much as possible of the accessible domain of osmotic pressures once equilibrium is reached. The sample tubes were conserved at 4 °C and cycles of centrifugation were done to accelerate homogenisation. Equilibrium is reached when water activity is the same in coexisting lamellar and polymer phases, which is easily deduced by observing the tubes characterised by a viscous and slightly turbid solution on top of a transparent polymer solution. Osmotic equilibrium also implies that *some* lecithin or Simulsol species are to be found in the polymer solution. The corresponding concentrations are, however, expected to be in the order of their respective critical micellar-aggregation-concentrations, viz. quite low. Neglecting the amount of "lost" material in computing the lamellar phase lipid fraction, as well as neglecting the contribution of lipid aggregates to osmotic pressure are therefore safe approximations.

Appendix A.3. Small-angle X-ray scattering

The small-angle scattering experiments were carried out at the Institute of Physics, University of São Paulo, Brazil, with the Xeuss instrument form Xenocs equipped with a Pilatus 300K detector (Dectris). Radiation produced by the microfocus Copper source is collected with a single-reflection multilayer optic producing a low-divergence, monochromatic beam with wavelength $\lambda = 0.154$ nm that is further collimated by a pair of scatterless slits-upstream slits 0.6×0.6 mm, downstream slits 0.5×0.5 mm. The sample-to-detector distance, calibrated with a Silver Behenate standard, is 0.77 m. Detector images span in practice a scattering wave vector range extending from $0.04\,\mathrm{nm}^{-1}$ to $3.5\,\mathrm{nm}^{-1}$. Samples are held in glass capillaries with a nominal diameter of 1.5 mm, and the scattering intensity is corrected for background by subtracting the properly normalised signal of a capillary filled with pure water. Exposure time varies from 15 up to 30 minutes, depending on the polymer solution concentration.

References

1. T. Gulik-Krzywicki, E. Rivas, V. Luzzati, J. Mol. Biol. **27**, 303 (1967).
2. D.M. LeNeveu, R.P. Rand, V.A. Parsegian, D. Gingell, Biophys. J. **18**, 209 (1977).
3. W. Helfrich, Z. Naturforsch **33a**, 305 (1978).
4. D.M. LeNeveu, R.P. Rand, V.A. Parsegian, Nature **259**, 601 (1976).
5. V.A. Parsegian, N. Fuller, R.P. Rand, Proc. Natl. Acad. Sci. U.S.A. **76**, 2750 (1979).
6. C.R. Safinya, D. Roux, G.S. Smith, S.K. Sinha, P. Dimon, N.A. Clark, A.-M. Bellocq, Phys. Rev. Lett. **57**, 2718 (1986).
7. T. Salditt, C. Li, A. Spaar, U. Mennicke, Eur. Phys. J. E **7**, 105 (2002).
8. F. Nallet, D. Roux, J. Prost, J. Phys. (Paris) **50**, 3147 (1989).
9. P. Richetti, P. Kékicheff, J.L. Parker, B.W. Ninham, Nature **346**, 252 (1990).
10. T. Pott, A. Colin, L. Navailles, D. Roux, Interface Sci. **11**, 249 (2003).
11. E. Andreoli de Oliveira, E.R. Teixeira da Silva, A. Février, É. Grelet, F. Nallet, L. Navailles, EPL **91**, 28001 (2010).
12. E.R. Teixeira da Silva, E. Andreoli de Oliveira, A. Février, F. Nallet, L. Navailles, Eur. Phys. J. E **34**, 83 (2011).
13. B.B. Gerbelli, R.L. Rubim, E.R. Silva, F. Nallet, L. Navailles, C.L.P. Oliveira, E.A. de Oliveira, Langmuir **29**, 13717 (2013).
14. K. Bougis, R. Leite Rubim, N. Ziane, J. Peyencet, A. Bentaleb, A. Février, C.L.P. Oliveira, E. Andreoli de Oliveira, L. Navailles, F. Nallet, Eur. Phys. J. E **38**, 78 (2015).

15. V. Luzzati, H. Mustacchi, A. Skoulios, F. Husson, Acta Crystallog. **13**, 660 (1960).
16. V. Luzzati, F. Husson, J. Cell Biol. **19**, 207 (1962).
17. F. Reiss-Husson, J. Mol. Biol. **25**, 363 (1967).
18. R. Lipowsky, S. Leibler, Phys. Rev. Lett. **56**, 2541 (1986).
19. R. Podgornik, V.A. Parsegian, Langmuir **8**, 557 (1992).
20. S.T. Milner, D. Roux, J. Phys. I **2**, 1741 (1992).
21. D. Bücker, W. Wagner, J. Phys. Chem. Ref. Data **35**, 205 (2006).
22. J.C. Maxwell, Nature **10**, 477 (1874).
23. J.E. Mayer, J. Chem. Phys. **5**, 67 (1937).
24. J.E. Jones, Proc. R. Soc. London A **106**, 463 (1924).
25. J. Israelachvili, H. Wennerström, Langmuir **6**, 873 (1990).
26. J. Israelachvili, H. Wennerström, J. Phys. Chem. **96**, 520 (1992).
27. J. Israelachvili, H. Wennerström, Nature **379**, 219 (1996).
28. E. Sparr, H. Wennerström, Curr. Opin. Colloid Interface Sci. **16**, 561 (2011).
29. E. Schneck, F. Sedlmeier, R.R. Netz, Proc. Natl. Acad. Sci. U.S.A. **109**, 14405 (2012).
30. M. Kanduč, A. Schlaich, E. Schneck, R.R. Netz, Advances Colloid Interface Sci. **208**, 142 (2014).
31. S. Marčelja, N. Radić, Chem. Phys. Lett. **42**, 129 (1976).
32. G. Cevc, R. Podgornik, B. Žekš, Chem. Phys. Lett. **91**, 193 (1982).
33. J.W. Cahn, J.W. Hilliard, J. Chem. Phys. **28**, 258 (1958).
34. P. Richetti, L. Moreau, P. Barois, P. Kékicheff, Phys. Rev. E **54**, 1749 (1996).
35. V.A. Parsegian, T. Zemb, Curr. Opin. Colloid Interface Sci. **16**, 618 (2011).
36. P. Bauduin, T. Zemb, Curr. Opin. Colloid Interface Sci. **19**, 9 (2014).
37. S.H. Donaldson Jr., A. Røyne, K. Kristiansen, M.V. Rapp, S. Das, M.A. Gebbie, D.W. Lee, P. Stock, M. Valtiner, J. Israelachvili, Langmuir **31**, 2051 (2015).
38. See, for instance, C. Kittel, H. Kroemer, in *Thermal Physics*, 2nd edition (W.H. Freeman and Co, New-York, 1980).